

# Gravitational waves and tadpole resummation: Efficient and easy convergence of finite temperature QFT

---

David Curtin<sup>a</sup>, Jyotirmoy Roy<sup>a</sup>, Graham White<sup>b</sup>

<sup>a</sup>*Department of Physics, University of Toronto, Toronto, Ontario, M5S 1A7, Canada*

<sup>b</sup>*Kavli IPMU (WPI), UTIAS, The University of Tokyo, Kashiwa, Chiba 277-8583, Japan*

**ABSTRACT:** We demonstrate analytically and numerically that “optimized partial dressing” (OPD) thermal mass resummation, which uses gap equation solutions inserted into the tadpole, efficiently tames finite temperature perturbation theory calculations of the effective thermal potential, without necessitating use of the high-temperature approximation. An analytical estimate of the scale dependence for OPD resummation, standard Parwani Daisy-resummation and dimensional reduction shows that OPD has similar scale dependence to dimensional reduction, greatly improved over Parwani resummation. We also elucidate how to construct and solve the gap equation for realistic numerical calculations, and demonstrate OPD’s improved accuracy and precision for a toy scalar model. An example of the physical significance of OPD’s improved accuracy is the maximal gravitational wave amplitude that a model is capable of generating, which Parwani resummation underestimates by two orders of magnitude. This highlights the need to bring theoretical uncertainties under control even when analysing broad features of a model. Given the simplicity of the OPD compared to two loop dimensional reduction, as well as the ease with which this scheme handles departures from the high temperature expansion, we argue this scheme has great potential in analyzing the parameter space of realistic BSM models.

---

## Contents

<b>1</b>	<b>Introduction</b>	<b>1</b>
<b>2</b>	<b>Perturbation theory at finite temperature and resummation methods</b>	<b>4</b>
<b>3</b>	<b>Review of gravitational wave signal calculation</b>	<b>7</b>
<b>4</b>	<b>Analytic comparison of resummation methods for <math>\phi^4</math> theories</b>	<b>8</b>
4.1	Single-field $\phi^4$ theory	9
4.1.1	Parwani resummation	10
4.1.2	Dimensional reduction	11
4.1.3	Gap resummation	12
4.2	Two-field $\phi^4$ -theory	13
4.2.1	Parwani resummation	14
4.2.2	Dimensional reduction	15
4.2.3	Gap resummation	17
<b>5</b>	<b>Numerical Implementation of Gap Resummation and Results</b>	<b>17</b>
5.1	Construction and solution of gap equation away from origin	18
5.2	Numerical results for benchmark two-field $\phi^4$ theory	19
<b>6</b>	<b>Discussion and conclusion</b>	<b>23</b>
<b>A</b>	<b>Loop level matching</b>	<b>24</b>
<b>B</b>	<b>2-loop Sunset diagram</b>	<b>26</b>

---

## 1 Introduction

A key aim of next generation experiments is to reveal the nature of cosmological electroweak symmetry breaking. It is expected that future colliders could definitively rule out or confirm a strong first order electroweak phase transition [1–4]. This departure from thermal equilibrium could supply one of the necessary ingredients for baryogenesis, explaining why there is more matter than anti-matter [5–9], and produce a stochastic gravitational wave background [3, 10–35] that can be measured by LISA [36] and other experiments in the mHz to kHz frequency range [37–42]. Besides this, strong phase transitions can appear in hidden sectors [43–53], symmetry breaking chains in grand unified gauge theories [54–58], conformal extensions of standard model [59, 60] and any number of other motivated scenarios [61]. In all cases, a proper treatment of perturbation theory is needed in order to make the theory predictive.

Unfortunately, 4D perturbation theory converges slowly at finite temperature (for a recent discussion of the convergence see ref [62]). Naively, the distribution function diverges for long wave length modes [63]. This issue is delayed if the theory is resummed such that the strongly coupled, long wave length behaviour is screened by hard thermal loops [64, 65]. However, even after such a “Daisy resummation” the perturbation theory converges slowly and as a result a one loop calculation can predict a peak gravitational wave amplitude that varies by multiple orders of magnitude [14, 66] for reasonable choices of the renormalization scale.

A known solution is to integrate out heavy Matsubara modes, which results in a 3D effective field theory. If one defines such a theory, both in its matching and the expansion in the dimensionally reduced theory, at next to leading order in the appropriate coupling constant,<sup>1</sup> the uncertainty in the gravitational wave spectrum can in some cases be reduced to the percent level [14]. Further, recent work has demonstrated that such perturbative calculations in the dimensionally reduced theory reproduce 3D lattice results very well, indicating that the infrared problems at higher loop may not be numerically important [67, 68].<sup>2</sup> The difficulty in dimensional reduction is its tractability. For even the Standard Model effective theory, defining the effective potential at noticeably better accuracy than (convenient) standard 4D methods requires the calculation of  $O(10^2)$  diagrams at finite temperature. While a recent package adds automation to this process [69], one still has to monitor whether it is appropriate to have multiple dynamical fields and whether to use the soft or ultrasoft potential for different regions of the parameter space. Further, it is difficult to go beyond the high temperature expansion in dimensional reduction as there is no longer a hierarchy between the lightest Matsubara mode and the soft scale to justify an effective field theory. This is an important limitation, since strong phase transitions require sizable couplings to the scalar undergoing the transition, which in turn leads to large field-space dependencies for particle masses and hence breakdowns in the high-temperature expansion. Therefore, it is strongly motivated to find more convenient 4D calculational methods that can achieve similar levels of accuracy. This would be of significant utility in examining the large theory space of BSM scenarios with strong phase transitions, electroweak or hidden.

One candidate for such a resummation method, called “partial dressing”, was first developed three decades ago [70] (see also [71–74]) in the context of simple a  $\phi^4$  toy model. It represented a simple analytical way of resumming the most important higher order corrections to the thermal propagator without double counting. More recently, this method was revisited and adapted for numerical application to the full SM with an additional scalar [75]. Referred to as “optimized partial dressing” (OPD), this method was also

---

<sup>1</sup>There is something of an inconsistency in the literature as to what prescription corresponds to what order. We will use the convention in this paper that next to leading order (NLO) is when a calculation is performed accurately in dimensional reduction to  $O(g^4)$ , such that performing the resummation at NLO and calculating the effective potential at NLO within the effective theory corresponds to correctly defining the theory up to  $O(g^4)$ .

<sup>2</sup>Two caveats deserve to be mentioned. First the time scale of the phase transition had strong uncertainties in the NLO dimensionally reduced theory. Second, the power counting used is slightly different to what has been used before, expanding in the ratio of the quartic coupling to the gauge coupling,  $x \sim \lambda/g^2$ , rather than the gauge coupling  $g^2$ .

shown to be easily applied outside of the finite temperature approximation, promising a more accurate treatment of strong phase transitions in this important regime. However, significant further work is required before OPD could become a gold standard for finite-temperature calculations. A systematic and rigorous study of the scheme’s convergence and validity is outstanding. There are open questions on the detailed analytical construction of the gap equation as a function of scalar vev, and the method of its numerical solution.<sup>3</sup> Finally, gauge bosons were not yet consistently included in the system of gap equations, and OPD’s relationship to RG improvement of the effective potential is unclear. Our work takes the first steps in addressing these issues, in particular the first two questions in the scenario where only one field acquires a vev during the transition.

The OPD scheme consists of two steps. The dominant contributions from many higher order diagrams are conveniently included in a gap equation for the thermal mass. The convenience arises from the fact that the diagrams do not need to be evaluated analytically, one merely needs to solve the gap equation, analytically in some approximations but generally numerically. It is also straight forward to handle cases where the high temperature expansion breaks down as one can merely use the full one loop thermal functions within the gap equation. The second step involves inserting the full thermal mass into the tadpole, rather than the full one loop effective potential as it was rigorously demonstrated that this is the way to prevent double counting of higher order diagrams [70]. Finally, missing diagrams are easily identified and can be added by hand. Apart from convenience and handling cases where the high temperature expansion breaks down, it is interesting to note that a (non-standard) dimensional reduction calculation *with gap resummation* finds a critical Higgs mass at which electroweak symmetry begins to become first order [76] as well as a critical end point in QCD at finite density [77], unlike standard dimensional reduction or 4D perturbative calculations. This suggests solving the gap equation may even be the missing ingredient to accurately characterize the SM phase diagram within a perturbative treatment.

In this paper we test the convergence of OPD in two simple test models - a single-field  $\phi^4$  theory, and a two-field  $\phi^4$  scalar field theory with a discrete  $Z_2 \times Z_2$  symmetry, only one of which is broken. We show a significant improvement both analytically and numerically to the convergence of perturbation theory compared with traditional methods (Daisy Resummation). Specifically, we compute the thermal potential near the critical temperature, compute the nucleation temperature and strength of the gravitational wave signal, and evaluate the dependence of these predictions on the renormalization scale to assess the degree of convergence. For the  $\phi^4$  theory we can furthermore demonstrate that the convergence of perturbation theory compares favourably even to NLO dimensional reduction. For the two-field  $\phi^4$  theory, a strong phase transition only occurs in regions of parameter space where the high-temperature expansion breaks down. As such, the standard

---

<sup>3</sup>In fact, the “optimized” part in OPD refers to the realization that the full finite-temperature thermal functions can be used in the potential while maintaining use of the high-temperature approximation in the gap equations to make their solution tractable, as well as the particular way mass derivatives are included in the gap equation away from the origin to find sensible  $M^2(\phi)$  trajectories. The latter part will be refined in this work.

dimensional reduction calculation fails and we cannot compare it to our 4D results, but this just serves to illustrate the utility in being able to go beyond the high-temperature approximation. Reduced scale dependence and the simple fact that that additional sizeable diagrams are included demonstrates that the OPD calculation is more precise and more accurate, respectively, than the standard 4D result.

Our simple test calculation can be seen as either obtaining results for a particularly simple hidden sector that undergoes a strong phase transition, or as a toy-model for SM extensions with extra scalars that achieve a strong electroweak phase transition. At any rate, obtaining careful results for this simple scenario allowed us to improve and more completely understand several analytical and numerical aspects of the OPD method, setting the stage for future work to develop OPD with the same level of rigor to include fermions, gauge bosons, RG-improved potentials and non-renormalizable operators in the Lagrangian.

The structure of this paper is as follows. In Sec. 2 and 3, we review the different resummation schemes in perturbative finite temperature field theory and computation of the gravitational wave signal. In Sec. 4, we study analytically the scale dependence of physical predictions in the  $\phi^4$  theory and the two scalar field theory. The numerical implementation and analysis, including detailed construction of the gap equation away from the origin, is discussed in Sec. 5. We finally conclude our paper with a discussion in Sec. 6.

## 2 Perturbation theory at finite temperature and resummation methods

In this section we briefly review finite temperature perturbation theory and the different resummation schemes we compare in this paper.

The form of gravitational wave spectra generated by a cosmological first order phase transition ends up being quite sensitive to the precise description of the effective potential. For example, in the case of the Standard Model Effective Field Theory or simple SM extensions with scalars, in regions where the theory has a strong phase transition the uncertainty in the peak gravitational wave amplitude can be multiple orders of magnitude [14, 66, 66].

The large uncertainty can be understood in two steps. First, finite temperature two loop (and sometimes higher order) contributions can be similar in size to zero temperature one loop pieces. Second, any modest uncertainty in the temperature at which a phase transition occurs is amplified substantially in the prediction of gravitational wave observables. To see the second point, consider that the peak amplitude of a gravitational wave spectrum from a cosmic phase transition (see Sec. 3) scales as

$$\Omega_{\text{GW}} \sim \alpha^2 (\beta/H_*)^{-2} \quad (2.1)$$

where  $\alpha \sim \Delta V/T^4$  is the change in the trace anomaly and  $\beta/H_*$  is the inverse time scale of the transition [78–81]. The difference in pressure between the two phases,  $\Delta V$ , tends to decrease with temperature and, from dimensional analysis, may typically scale quartically with the inverse temperature. The inverse time scale typically scales exponentially, so if the uncertainty in  $T$  is not too large one can take this as scaling linearly with the inverse temperature. Altogether, this accounts for a remarkable scaling relationship for the peak

amplitude

$$\Omega_{\text{GW}} \sim T^{-18} \quad (2.2)$$

such that an  $O(25\%)$  uncertainty in the percolation temperature can lead to two orders of magnitude uncertainty in gravitational wave observables.

The parameters responsible for producing a gravitational wave amplitude can independently be constrained by measurements at future colliders. However, if the gravitational wave observables are to provide meaningful constraints on the parameters, the theoretical uncertainties need to be brought under control. In fact, as we will later see, even broad questions about a model such as “what is the largest possible gravitational wave amplitude consistent with this model across its parameter space” can vary by orders of magnitude comparing crude and more sophisticated calculation techniques.

We follow standard procedure in attempting to measure the importance of neglected higher order terms by measuring the renormalization scale dependence of various observables [14]. In doing so one needs to make a somewhat arbitrary choice of what range of values for the renormalization scale one should use in the loop calculation. However, even the generous range for the scale parameter considered in [66] can have the next to leading order predictions not enveloped within the uncertainty bands of the leading order prediction. Our analysis should therefore give a meaningful idea of the calculation’s convergence.

The conventional resummation methods that result in these large theoretical uncertainties were developed by Parwani [65] as well as Arnold and Espinosa [64]. In these schemes, the long distance behaviour is screened by including a thermal mass term,  $\Pi$ , such that the resummed potential has the form

$$V_{1\text{-loop}}(M^2) \rightarrow V_{1\text{-loop}}(M^2 + \Pi) . \quad (2.3)$$

The thermal mass and the finite-temperature one-loop potential are readily calculated using standard methods.<sup>4</sup> It is useful to recall the form of  $\Pi$  in the high-temperature expansion for a  $\phi^4$  theory with quartic coupling  $g$ :

$$\Pi \sim g^2 T^2 - \frac{g^2 T M}{8\pi} - \frac{g^2 M^2}{32\pi^2} \log \frac{\mu^2}{T^2} + \dots \quad (2.4)$$

The two traditional resummation schemes differ in some details. Arnold-Espinosa adds a ring-term to the effective potential, which can be found by performing the substitution in Eqn. (2.3) in the high-temperature-expanded thermal potential only. Parwani, on the other hand, substitutes  $M^2 + \Pi$  into the full effective potential, including the zero-temperature Coleman-Weinberg potential. For reasons that are beyond the scope of this quick discussion, the field tended to use the Arnold-Espinosa scheme, but the Parwani scheme actually has better scale dependence, since the thermal mass contribution in the zero-temperature Coleman-Weinberg piece induces a partial cancellation with the finite-temperature potential piece. We therefore use the Parwani scheme to minimize the scale dependence of

---

<sup>4</sup>See e.g. [82], or [75] for a brief summary using the same notation and conventions as our analysis.

traditional Daisy resummation, leading to the most conservative assessment of the benefits of OPD or DR.

The Parwani resummation scheme correctly reorganizes the theory such that all pieces up to third order in the  $SU(2)_L$  gauge coupling or larger are included in the potential. However,  $g_2$  is reasonably large in the Standard Model, and terms at least in the next order  $\mathcal{O}(g_2^4)$  are needed to bring uncertainties in the gravitational wave amplitude under control. Organizing perturbation theory with Parwani resummation to include all terms of  $\mathcal{O}(g_2^4)$  is highly non trivial, as naive methods lead to double counting.

To improve the accuracy of finite temperature perturbation theory, dimensional reduction at next to next to leading order appears to provide a recipe, reducing theoretical uncertainties to the percent level [14]. Dimensional reduction relies on the observation that in imaginary time, the quantum field theory is identical to a three dimensional theory with a compactified time dimension whose size is determined by the temperature [83]. One can then integrate out the heavy Kaluza-Klein like modes, known as Matsubara modes, leaving an effective field theory in three dimensions. If a scale hierarchy persists between the remaining states, typically a soft and ultrasoft scale of order  $gT$  and  $g^2T/\pi$  respectively, the soft states can be integrated out leaving behind a simpler effective field theory again.

Dimensional reduction naturally incorporates resummation through the matching relations between the four dimensional theory and the effective dimensionally reduced theory. Calculating the relevant self energy diagrams in these matching relations can be done at multi-loop levels of accuracy in addition to defining the effective potential at multiple loops within the effective theory without double counting. The whole process makes it straightforward albeit work intensive to organize perturbation theory into powers of an effective coupling constant (or a ratio of constants as argued for in ref. [68]). At next to leading order (or  $\mathcal{O}(g^4)$ ) the theoretical uncertainties in the gravitational wave amplitude for the Standard Model Effective Field Theory are effectively under control. The drawback of dimensional reduction is both the enormous practical difficulty of the scheme - over a hundred diagrams are required to see noticeable improvement compared with conventional methods - and the fact that it conventionally assumes the validity of the high temperature expansion.

Another method of resummation - partial dressing or gap resummation - calculates many higher order diagrams numerically by solving a gap equation, which can be pictorially represented as follows:

$$\text{Double Line} = \text{Single Line} + \text{Single Line with Self-Energy Loop} + \text{Single Line with Tadpole Loop}$$

where the double lines represent the resummed mass and the single line the tree level mass. It was demonstrated three decades ago [70] that in order to avoid double counting of higher

order diagrams, one needs to insert the resummed mass into the tadpole and integrate,

$$V = \int d\phi \left[ \frac{\partial V_{1\text{-loop}}(M^2)}{\partial \phi} + \frac{\partial V_{\text{sun}}(M^2)}{\partial \phi} \right] \quad (2.5)$$

where the first term,  $V_{1\text{-loop}}$ , is the zero plus finite temperature one loop potential and the second term is the finite temperature potential due to two loop sunsets. This term is neglected in the solution to the gap equation. The method can also be applied when the high temperature regime breaks down, in particular by keeping the high-temperature approximation in the gap equation but using full thermal integrals in the potential [75] (referred to as “Optimized Partial Dressing” (OPD)), and is much easier to use than dimensional reduction as the gap equation only requires one to define the one loop effective potential at finite temperature. It is therefore highly attractive if it can be demonstrated to provide substantial improvement over conventional methods, i.e. Parwani resummation. In this work, we seek to ascertain systematically for the first time whether gap resummation, or OPD, performs better than Parwani resummation and is comparably to dimensional reduction at next to leading order for the purposes of obtaining gravitational wave predictions. We also clarify how the gap equation should be constructed and numerically solved away from the origin.

### 3 Review of gravitational wave signal calculation

Any uncertainties in the prediction of the thermal potential, arising from the slow convergence of perturbation theory at finite temperature, become amplified when calculating the gravitational wave observables. In this section we will review the calculation of the gravitational wave peak amplitude due to the acoustic contribution calculated using the sound shell model [84–87]. We will later consider the two scalar field model and assume that the Standard Model particle content is coupled strongly enough to maintain kinetic equilibrium with our two new scalar fields but weakly enough that we can ignore their effect on the gravitational wave phenomenology. In the sound shell model, the spectrum is completely determined by the temperature of the transition, the fluid velocity, the mean bubble separation, the life time of the sound waves and the fraction of energy released that becomes converted to sound waves. To a good approximation, these quantities can be related to four macroscopic parameters - the transition temperature, the bubble wall velocity, the trace anomaly normalized by the critical density

$$\alpha = \frac{\Delta V - T d\Delta V/dT}{\rho_c} \quad (3.1)$$

and the inverse lifetime of the transition

$$\frac{\beta}{H_*} = T \frac{d(S_E/T)}{dT} . \quad (3.2)$$

A more diligent calculation irones out errors that are orthogonal to our analysis [88] so we ignore them in this work. It should be noted, however that in the sound shell model, the



four thermal parameters result in two observables, the peak amplitude and frequency. More careful simulations yield a more optimistic picture where all four thermal parameters can be extracted from the precise shape of the power spectrum [89], but conservative analyses claim fits to three parameters [90]. In any case, the sound shell model predicts a spectral shape, of the form

$$S_{\text{SW}}(f) = \left( \frac{f}{f_{\text{SW}}} \right)^3 \left[ \frac{7}{4 + 3(f/f_{\text{SW}})^2} \right]^{7/2}, \quad (3.3)$$

with a peak frequency

$$f_{\text{SW}} = 1.9 \times 10^{-5} \frac{1}{v_w} \left( \frac{\beta}{H_n} \right) \left( \frac{T_n}{100 \text{ GeV}} \right) \left( \frac{g_*}{100} \right)^{1/6} \text{ Hz}, \quad (3.4)$$

and a peak amplitude [80, 84–87]

$$h^2 \Omega_{\text{GW}} = 8.5 \times 10^{-6} \left( \frac{100}{g_*} \right)^{1/3} \kappa^2 \left( \frac{H_*}{\beta} \right) v_w \Upsilon(\bar{U}_{f,\text{max}}, R_*) , \quad (3.5)$$

where  $v_w$  is the bubble wall velocity and  $g_*$  counts the number of relativistic degrees of freedom in the plasma at the time of transition. For the efficiency we assume a relativistic bubble wall velocity which means we can, to a good approximation, relate the trace anomaly to the kinetic energy fraction

$$\kappa \simeq \frac{\alpha}{0.73 + 0.083\sqrt{\alpha} + \alpha} \quad (3.6)$$

and the suppression factor from the finite lifetime of the source is

$$\Upsilon = 1 - \frac{1}{\sqrt{1 - 2\tau_{\text{SW}} H_s}}, \quad (3.7)$$

where  $\tau_{\text{SW}} = R_*/\bar{U}_f$  with the fluid velocity and the mean bubble separation having the form  $U_f^2 \sim \frac{3}{4}\kappa\alpha$  and  $R_* = (8\pi)^{1/3}v_w/\beta$ , respectively. Finally, to derive the percolation temperature  $T_p$  one has to solve the equation,

$$\frac{S_3(T_p)}{T_p} = 131 - \log(A/T^4) - 4 \log \left( \frac{T}{100 \text{ GeV}} \right) - 4 \log \left( \frac{\beta(T)/H}{100} \right) + 3 \log(v_w). \quad (3.8)$$

#### 4 Analytic comparison of resummation methods for $\phi^4$ theories

Conceptually, in this paper we compute the effective potential at one-loop *fixed order* in the couplings, with either Parwani or OPD thermal mass resummation. (We leave a careful treatment of RG-improved potentials and thermal resummation to a future investigation.) Working in the  $\overline{\text{MS}}$  regularization scheme, which includes an arbitrary renormalization scale  $\mu$ , this specifically involves picking a value of  $\mu$ , computing measured experimental observables and picking parameters to reproduce these observables, and then computing new predictions like the thermal potential. An all-orders calculation would yield predictions

that are independent of  $\mu$ , but any truncated perturbative calculation will introduce  $\mu$ -dependence in the predictions due to the missing contributions, meaning that different choices of renormalization scale yield (after re-matching the theory) to different predictions. Standard RG arguments tell us that the true expansion parameter of the theory includes not just the fixed-order coupling, but also logarithms of  $\mu$  and various mass scales. Therefore, a sensible choice of  $\mu$  close to the most important mass scale is expected to yield the most accurate result with the smallest  $\mu$ -dependence. (Note that this choice of mass scale is not unambiguous even at zero temperature, and at finite temperature there may be no clear choice that minimizes scale dependence.) Furthermore, the size of this  $\mu$ -dependence is expected to give an indication of the size of the missing contributions, and therefore the degree of convergence and precision of the perturbative calculation.

The above is exactly how we assess the convergence of the fully numerical calculation in Sec. 5, with the predictions for each different choice of  $\mu$  being obtained by re-matching the theory for different renormalization scales and repeating the fixed-order calculation with thermal resummation.

In this section, our aim is to perform a more limited but analytical version of this calculation, to transparently demonstrate that OPD has smaller scale dependence than standard Parwani thermal resummation and is comparable to dimensional reduction. This can be done by letting RG evolution take the place of re-matching the theory for different values of  $\mu$ , since the RG takes into account the changing coupling at different energy scales (up to a small finite piece). Specifically, we compute various aspects of the effective potential at the origin, taking into account the implicit scale dependence by using running couplings as a function of  $\mu$  in the potential, which are obtained by matching at a single scale with RG-improved tree-level accuracy, similar to [66]. The implicit scale dependence in the running couplings should cancel the explicit scale dependence in the loop corrections, with the residual uncanceled piece being parametrically the same size as the next order in perturbation theory. If the residual dependence of any observable on the renormalization scale is severe, then the theory has not been defined accurately enough and higher order corrections need to be included. This residual dependence can then be straightforwardly compared across different calculational schemes.

#### 4.1 Single-field $\phi^4$ theory

Let us consider a simple real  $\phi^4$  theory with a discrete  $Z_2$  symmetry. This theory admits phase transitions that are ultimately too weak to consider the gravitational wave phenomenology. However, the simplicity also makes the differences between the resummation schemes in obtaining predictions for the thermal potential transparent, and will serve as a useful pedagogical warm up. The tree-level potential has the form

$$V_0 = \frac{m^2}{2}\phi^2 + \frac{g^2}{4!}\phi^4 . \quad (4.1)$$

The one loop correction at zero temperature in addition to the tree level potential gives the Coleman-Weinberg potential,

$$V_{\text{CW}} = \frac{M^4}{64\pi^2} \left( \log \left[ \frac{M^2}{\mu^2} \right] - \frac{3}{2} \right) , \quad (4.2)$$

where  $\mu$  is the renormalization scale in the  $\overline{\text{MS}}$  scheme and  $M^2 = m^2 + g^2\phi^2/2$  is the field dependent mass. No physical quantity will depend on the choice of the renormalization scale. Therefore, the above dependence is merely an artefact of the truncation of perturbation theory at finite order. As such, a convenient measure for the convergence of perturbation theory is the residual scale dependence - the implicit scale dependence arising from running couplings in the tree level potential should cancel the explicit scale dependence in the Coleman-Weinberg potential leaving corrections from the implicit scale dependence in the latter term which is formally higher order. Let us demonstrate this explicitly. Our renormalization group equations at one loop have the form

$$\mu \frac{dm^2}{d\mu} = \frac{g^2 m^2}{16\pi^2} \quad (4.3)$$

$$\mu \frac{dg^2}{d\mu} = \frac{3g^4}{16\pi^2} . \quad (4.4)$$

The scale dependence of our potential to  $O(g^4)$  then has the form

$$\mu \frac{dV_0}{d\mu} = \frac{g^2 m^2}{32\pi^2} \phi^2 + \frac{g^4}{128\pi^2} \phi^4 \quad (4.5)$$

$$\mu \frac{dV_{\text{CW}}}{d\mu} = -\frac{M^4}{32\pi^2} \quad (4.6)$$

which sums to a field independent cosmological constant that we can ignore.

At finite temperature, the one loop correction in the high temperature expansion has the form

$$V_{\text{T}} = \frac{1}{48} g^2 T^2 \phi^2 - T \frac{M^3}{12\pi} - \frac{M^4}{64\pi^2} \log \frac{M^2}{a_b T^2} . \quad (4.7)$$

where  $a_b = 16\pi^2 \exp(\frac{3}{2} - 2\gamma_E)$ ,  $\gamma_E$  being the Euler-Mascheroni constant. It is trivial to see that nothing in our one loop theory cancels the implicit scale dependence of the finite temperature piece. Moreover, the size of the uncanceled corrections are as large as the scale dependence of the tree level pieces in powers of  $g/\pi$  and could be relatively larger when  $T/\phi$  is large, that is the infrared limit. On top of the explicit infrared divergence that appears at higher loop, finite temperature perturbation theory converges slowly in part because of a mismatch of the order of the loop expansion and the size of a term in powers of  $g^n/\pi^m$  as well as the infrared enhancement of uncanceled pieces in terms of  $T/\phi$ .

#### 4.1.1 Parwani resummation

Historically, resumming daisy diagrams was to cure the infrared divergences inherent in finite temperature field theory [65]. However, since this means including higher loop diagrams in the effective potential, we will also see an improvement in the scale dependence. Parwani resummation (also known as Truncated Full Dressing (TFD) to distinguish it from OPD) works through replacing  $M^2 \rightarrow M^2 + \Pi$  where  $\Pi = \frac{1}{24} g^2 T^2$  is the thermal mass to lowest order in the high-temperature expansion. A partial cancellation of the scale

dependence occurs

$$\mu \frac{dV_T}{d\mu} \supset 3 \frac{g^4}{48 \times 16\pi^2} T^2 \phi^2 \quad (4.8)$$

$$\mu \frac{dV_{CW}}{d\mu} \supset -\frac{M^2 \Pi}{16\pi^2} \supset -\frac{g^4}{48 \times 16\pi^2} T^2 \phi^2 . \quad (4.9)$$

The opposite signs in the above terms is the origin of the cancellation. To achieve a full cancellation, we require the missing two loop term which is the sunset diagram. At high temperature it is

$$V_{\text{sun}} = -\frac{1}{12} g^4 \phi^2 \frac{3T^2}{32\pi^4} \left( \log \left[ \frac{\mu^2}{M^2} \right] + 2 \right) \left( \frac{\pi^2}{6} - \frac{\pi M}{2T} \right) . \quad (4.10)$$

In the above we have performed a high temperature expansion. The full expression that we use in our numerical calculation we put into Appendix B. A straight forward calculation shows that the scale dependence of the  $T^2 \phi^2$  term cancels. The leading order uncanceled piece is

$$\mu \frac{dV_{\text{TFD}}}{d\mu} = -\frac{g^2 T}{192\pi^2} (M^2 + \Pi)^{3/2} . \quad (4.11)$$

#### 4.1.2 Dimensional reduction

At finite temperature in the imaginary time formalism, a thermal field theory is equivalent to a Kaluza-Klein theory with a compactified imaginary time direction of size  $1/T$ . Integrating out this tower of Matsubara modes leaves one with an effective theory in three dimensions. Doing so automatically includes resummation by construction via the matching relations. Although famously rigorous and consistent, it can be quite formidable technically in a realistic model. In the case of  $\phi^4$  theory, the resulting effective potential is simple enough to be written in a closed form, even at NLO,

$$V_{\text{DR}} = T \left( \frac{1}{2} m_3^2 \phi_3^2 + \frac{1}{24} g_3^2 \phi_3^4 - \frac{1}{12\pi} (M_3^2)^{3/2} + \frac{1}{16\pi^2} \left( \frac{1}{8} g_3^2 M_3^2 \right) + \frac{1}{24} g_3^4 \phi_3^2 \frac{1}{16\pi^2} \left( 1 + 2 \log \left[ \frac{\mu_3}{3M_3} \right] \right) \right) \quad (4.12)$$

where

$$M_3^2 = m_3^2 + \frac{1}{2} g_3^2 v_3^2 \quad (4.13)$$

$$g_3^2 = T \left( g^2 - \frac{3}{32\pi^2} g^4 L_b \right) \quad (4.14)$$

$$m_3^2 = m^2 + \frac{1}{24} g^2 T^2 - \frac{1}{16\pi^2} \left( \frac{1}{2} g^2 m^2 L_b + \frac{1}{16} g^2 T^2 L_b + \frac{1}{6} g_3^4 (c + \log[3T/\mu_3]) \right) \quad (4.15)$$

$$v_3 = \frac{\phi}{\sqrt{T}} . \quad (4.16)$$

Here,  $\mu_3$  is the scale dependence in the effective theory and  $L_b = (\log[\mu^2/T^2] + 2\gamma_E - 2 \log 4\pi)$ . For a fair comparison, we take the larger of the dependencies on  $\mu_3$  and  $\mu$  as reflective of

the residual scale dependence at NLO. To calculate the dependence on the former, it is useful to write

$$\mu_3 \frac{dm_3^2}{d\mu_3} = \mu_3 \frac{dM_3^2}{d\mu_3} \frac{1}{96\pi^2} g^4 T^2 \quad (4.17)$$

$$\mu_3 \frac{dV_{\text{DR}}}{d\mu_3} \supset -\frac{1}{384\pi^2} g^4 T^2 \phi^2. \quad (4.18)$$

The dependence on  $\mu$  turns out to be subdominant and has the form

$$\mu \frac{dg_3^2}{d\mu} = O(g^6) \quad (4.19)$$

$$\mu \frac{dm_3^2}{d\mu} = \frac{m^2 g^2}{16\pi^2} + \frac{1}{24} \frac{3}{16\pi^2} g^4 T^2 - \frac{1}{16\pi^2} \left( \frac{1}{8\pi^2} g^4 m^2 L_b + g^2 m^2 + \frac{1}{8} g^4 T^2 \right) \quad (4.20)$$

$$\mu \frac{dm_3^2}{d\mu} = -\frac{1}{16\pi^2} \left( \frac{1}{8\pi^2} g^4 m^2 L_b \right), \quad (4.21)$$

so we focus on the  $\mu_3$  dependence and find

$$\mu_3 \frac{dV_{\text{DR}}}{d\mu_3} = -\frac{1}{768\pi^3} g^4 T^3 M_3. \quad (4.22)$$

This is of order  $g^4/\pi^3$ , much smaller than the  $\mathcal{O}(g^2)$  residual dependence of the Parwani calculation.

#### 4.1.3 Gap resummation

Higher order diagrams can be included in a simple gap equation where the thermal mass is defined as the second derivative of the resummed potential

$$M^2 = m^2 + \frac{g^2}{2} \phi^2 + \frac{g^2 T^2}{24} - \frac{g^2 T M}{8\pi} - \frac{g^2 M^2 L_b}{32\pi^2} - \frac{g^4 \phi^2 L_b}{32\pi^2}. \quad (4.23)$$

The resulting thermal mass cannot be substituted into the full potential without double counting diagrams. Instead, one includes the resummation of the tadpole

$$V'_{\text{OPD}} = g^2 \phi \left( \frac{T^2}{24} - \frac{T M}{8\pi} - \frac{M^2 L_b}{32\pi^2} \right) - \frac{g^4 \phi T}{64\pi^2} \left( \log \left[ \frac{\mu^2}{M^2} \right] + 2 \right) \left( \frac{\pi^2}{6} - \frac{\pi M}{2 T} \right) \quad (4.24)$$

and then integrates over the field to acquire the potential at the end. In the above, everything was written in the high temperature to make the problem analytically tractable. However, the power of gap resummation is that the gap equation can be solved numerically without a high temperature expansion. The scale dependence of the resummed mass and the tadpole can be written to  $O(g^4)$

$$\begin{aligned} \mu \frac{dV'_{\text{OPD}}}{d\mu} &= \frac{3}{16\pi^2} g^4 \phi \left( -\frac{T M}{8\pi} \right) + g^2 \phi \left( -\frac{T}{16\pi M} \mu \frac{dM^2}{d\mu} - 2 \frac{M^2}{32\pi^2} \right) + \frac{1}{384\pi^2} g^4 \phi T^2 - \frac{g^4 M T \phi}{64\pi^3} \\ \mu \frac{dM^2}{d\mu} &= -\frac{g^4 T M}{64\pi^3} - \frac{g^2 T}{8\pi M} \mu \frac{dM^2}{d\mu} + \frac{g^4}{128\pi^2} T^2. \end{aligned} \quad (4.25)$$

After substituting the derivative of the gap equation with respect to the scale into the scale dependence of the tadpole, the remaining scale dependence cancels up to  $O(g^4)$  and the residual piece is  $O(g^6)$ ,

$$\mu \frac{dV'_{\text{OPD}}}{d\mu} = -\frac{(1-\zeta)g^6 T^3 \phi}{192\pi^3 M} + \frac{g^6 T^2 \phi^2}{256\pi^3 M} \quad (4.26)$$

where  $\zeta = 0$  corresponds to the direct result of the above treatment, and  $\zeta = 1$  is obtained by including sunsets in the gap equation. Of course, this is the scale dependence of the tadpole, not the potential. After integration, the residual term is the same order as in DR with a slightly different prefactor, suggesting that the use of gap equations is competitive with NLO DR,

$$\mu \frac{dV_{\text{OPD}}}{d\mu} = \frac{g^4 M T^2 (8T(1-\zeta) + 3\phi)}{768\sqrt{3}\pi^3} - \frac{g^4 m^2 T^2 \phi}{256\sqrt{3}\pi^3 M}, \quad (4.27)$$

where we have, in the final term, expanded an arctanh function that is actually well behaved in the infrared limit.

## 4.2 Two-field $\phi^4$ -theory

Let us now consider a two scalar field model. In principle, this is the minimal model that could produce an observable gravitational wave signature, as the portal couplings can produce a modest thermal barrier. In practice, the peak amplitude tends to be very small. Nevertheless, the predictions of this model can be treated as realistic phenomenological predictions, perhaps existing in some dark sector, under the proviso that any couplings keeping the system in kinetic equilibrium with the visible sector can be sufficiently small that their effect on the potential is negligible. The potential for our model is

$$V_0 = \frac{1}{2}m_1^2\phi_1^2 + \frac{g_1^2}{4!}\phi_1^4 + \frac{1}{2}m_2^2\phi_2^2 + \frac{g_2^2}{4!}\phi_2^4 + \frac{g_{12}^2}{4}\phi_1^2\phi_2^2. \quad (4.28)$$

We will consider the case where the second scalar does not acquire a vev throughout the transition, as its function is to provide the thermal barrier. In this case the field dependent masses have the simple form

$$M_1^2 = m_1^2 + \frac{1}{2}g_1^2\phi_1^2 \quad (4.29)$$

$$M_2^2 = m_2^2 + \frac{1}{2}g_{12}^2\phi_1^2. \quad (4.30)$$

Note that we include  $\phi_2$  when performing derivatives with respect to the potential and only set  $\phi_2$  to zero at the end. To keep equations compact, we do not show their contribution

here. Finally, the renormalization group equations have the form

$$\mu \frac{dg_1^2}{d\mu} = \frac{3g_1^4}{16\pi^2} + \frac{3g_{12}^4}{16\pi^2} \quad (4.31)$$

$$\mu \frac{dg_2^2}{d\mu} = \frac{3g_{12}^4}{16\pi^2} + \frac{3g_2^4}{16\pi^2} \quad (4.32)$$

$$\mu \frac{dg_{12}^2}{d\mu} = \frac{g_1^2 g_{12}^2}{16\pi^2} + \frac{4g_{12}^4}{16\pi^2} + \frac{g_{12}^2 g_2^2}{16\pi^2} \quad (4.33)$$

$$\mu \frac{dm_1^2}{d\mu} = \frac{g_1^2 m_1^2}{16\pi^2} + \frac{g_{12}^2 m_2^2}{16\pi^2} \quad (4.34)$$

$$\mu \frac{dm_2^2}{d\mu} = \frac{g_{12}^2 m_1^2}{16\pi^2} + \frac{g_2^2 m_2^2}{16\pi^2} \quad (4.35)$$

#### 4.2.1 Parwani resummation

In the Parwani scheme, the thermal masses have the form

$$\Pi_1 = \frac{g_1^2 T^2}{24} + \frac{g_{12}^2 T^2}{24} \quad (4.36)$$

$$\Pi_2 = \frac{g_{12}^2 T^2}{24} + \frac{g_2^2 T^2}{24} . \quad (4.37)$$

Let us now put together the scale dependence of each piece of the potential in the Parwani regime. First the tree level potential,

$$\mu \frac{dV_0}{d\mu} = \frac{1}{128\pi^2} (4 (g_1^2 m_1^2 + g_{12}^2 m_2^2) \phi_1^2 + (g_1^4 + g_{12}^4) \phi_1^4) \quad (4.38)$$

and the zero temperature piece of the Coleman Weinberg has the form

$$\mu \frac{dV_{CW}}{d\mu} \supset -\frac{1}{128\pi^2} \left( (2m_1^2 + g_1^2 \phi_1^2)^2 + (2m_2^2 + g_{12}^2 \phi_1^2)^2 \right) . \quad (4.39)$$

The above piece cancels the field dependent part of the scale dependence of the tree level potential.

The quadratic temperature dependent piece has three parts. First from the high temperature expansion of the one loop potential, which at lowest order in the high-temperature expansion is

$$\mu \frac{dV_T}{d\mu} \supset \frac{T^2}{768\pi^2} (3g_1^4 + 7g_{12}^4 + g_1^2 g_{12}^2 + g_2^2 g_{12}^2) \phi_1^2 . \quad (4.40)$$

This partially cancels the piece arising from the thermal masses in the Coleman Weinberg potential

$$\mu \frac{dV_{CW}}{d\mu} \supset -\frac{T^2}{768\pi^2} (g_1^4 + g_1^2 g_{12}^2 + g_{12}^4 + g_{12}^2 g_2^2) \phi_1^2 . \quad (4.41)$$

Adding the two terms together leads to a residual piece

$$\mu \frac{d(V_T + V_{CW})}{d\mu} \supset \frac{g_1^4 + 3g_{12}^4}{384\pi^2} T^2 \phi_1^2 - \frac{g_1^2 m_1^2 \bar{M}_1 T + g_{12}^2 m_1^2 \bar{M}_2 T + g_{12}^2 m_2^2 \bar{M}_1 T + g_2^2 m_2^2 \bar{M}_2 T}{128\pi^3} . \quad (4.42)$$

with  $\bar{M}_i^2 = M_i^2 + \Pi_i$ , and we also show the next-to-leading  $\mathcal{O}(T)$  part of the high-temperature expansion for reasons that will become clear. The final contribution is from the leading power sunset term, which in the high temperature expansion has the form

$$\begin{aligned} V_{\text{sun}} = & -\frac{3T^2}{32\pi^4} \frac{g_1^4}{12} \phi_1^2 \left( \log \left[ \frac{\mu^2}{\bar{M}_1^2} \right] + 2 \right) \left( \frac{\pi^2}{6} - \frac{\pi}{2} \frac{\bar{M}_1}{T} \right) \\ & -\frac{2T^2}{32\pi^4} \frac{g_{12}^4}{4} \phi_1^2 \left( \log \left[ \frac{\mu^2}{\bar{M}_2^2} \right] + 2 \right) \left( \frac{\pi^2}{6} - \frac{\pi}{2} \frac{\bar{M}_2}{T} \right) \\ & -\frac{T^2}{32\pi^4} \frac{g_{12}^4}{4} \phi_1^2 \left( \log \left[ \frac{\mu^2}{\bar{M}_1^2} \right] + 2 \right) \left( \frac{\pi^2}{6} - \frac{\pi}{2} \frac{\bar{M}_1}{T} \right) . \end{aligned} \quad (4.43)$$

The sunset actually cancels the  $\mathcal{O}(T^2)$  term in Eqn. (4.42) completely, so we focus on the  $\mathcal{O}(T)$  contribution

$$\mu \frac{dV_{\text{sun}}}{d\mu} \supset \frac{g_1^4 \bar{M}_1 + g_{12}^4 (\bar{M}_1 + 2\bar{M}_2)}{128\pi^3} T \phi_1^2 . \quad (4.44)$$

The residual scale dependence in TFD is the sum of the  $\mathcal{O}(T)$  terms in Eqns. (4.42) and (4.44). If there is strong first order phase transition, we expect  $g_{12} \gg g_1, g_2$ . We therefore show the leading order field dependent term in powers of  $g_{12}$ :

$$\mu \frac{dV_{\text{TFD}}}{d\mu} = -\frac{g_{12}^2 (m_2^2 \bar{M}_1 + m_1^2 \bar{M}_2) T}{128\pi^3} . \quad (4.45)$$

The leading order uncanceled term is therefore of the same order as in the single field case.

#### 4.2.2 Dimensional reduction

We use DRalgo [69] to derive the potential for this model at  $\mathcal{O}(g^4)$ . That is we include 2-loop calculations in the dimensionally reduced theory and a NLO (two loop) resummation (NNLO in the nomenclature of DRalgo). For our analytic comparison, it is easiest to work with the soft rather than the ultrasoft potential, though the appropriate potential to use depends upon where one is in the parameter space. The full soft potential is

$$\begin{aligned} V_{3d} = & \frac{m_{1,3d}^2 \phi_{3d}^2}{2} + \frac{\lambda_{1,3d} \phi_{3d}^4}{24} - \frac{\left( m_{1,3d}^2 + \frac{\lambda_{1,3d} \phi_{3d}^2}{2} \right)^{3/2}}{12\pi} - \frac{\left( m_{2,3d}^2 + \frac{\lambda_{12,3d} \phi_{3d}^2}{2} \right)^{3/2}}{12\pi} \\ & + \frac{\lambda_{1,3d} \left( m_{1,3d}^2 + \frac{\lambda_{1,3d} \phi_{3d}^2}{2} \right)}{128\pi^2} + \frac{\lambda_{12,3d} \sqrt{m_{1,3s}^2 + \frac{\lambda_{1,3d} \phi_{3d}^2}{2}} \sqrt{m_{2,3s}^2 + \frac{\lambda_{12,3d} \phi_{3d}^2}{2}}}{64\pi^2} \\ & + \frac{\lambda_{2,3d} \left( m_{2,3s}^2 + \frac{\lambda_{12,3d} \phi_{3d}^2}{2} \right)}{128\pi^2} - \frac{\lambda_{1,3d}^2 \phi_{3d}^2 \left( \frac{1}{2} + \log \left[ \frac{\mu_3}{3\sqrt{m_{1,3s}^2 + \frac{\lambda_{1,3d} \phi_{3d}^2}{2}}} \right] \right)}{192\pi^2} \\ & + \frac{\lambda_{12,3d}^2 \phi_{3d}^2 \left( \frac{1}{2} + \log \left[ \frac{\mu_3}{\sqrt{m_{1,3s}^2 + \frac{\lambda_{1,3d} \phi_{3d}^2}{2}} + 2m_{2,3s}^2 + \frac{\lambda_{12,3d} \phi_{3d}^2}{2}} \right] \right)}{64\pi^2} . \end{aligned} \quad (4.46)$$



Here the dimensionally reduced couplings, masses and fields are given by

$$\lambda_{1,3d} = T \left( g_1^2 - \frac{3L_b(g_1^4 + g_{12}^4)}{32\pi^2} \right) \quad (4.47)$$

$$\lambda_{2,3d} = T \left( g_2^2 - \frac{3L_b(g_{12}^4 + g_2^4)}{32\pi^2} \right) \quad (4.48)$$

$$\lambda_{12,3d} = T \left( g_{12}^2 - \frac{L_b g_{12}^2 (g_1^2 + 4g_{12}^2 + g_2^2)}{32\pi^2} \right) \quad (4.49)$$

$$\begin{aligned} m_{1,3d}^2 = & m_1^2 + \frac{1}{24} T^2 (g_1^2 + g_{12}^2) \\ & - \frac{1}{768\pi^2} \left( L_b [24m_1^2 g_1^2 + 24m_2^2 g_{12}^2 + T^2 (-g_1^4 + g_1^2 g_{12}^2 + g_{12}^2 [-5g_{12}^2 + g_2^2])] \right. \\ & \left. + 4T^2 (g_1^4 + 3g_{12}^4) (\gamma_E - 12 \log A) - 8(3\lambda_{12,3d}^2 + \lambda_{1,3d}^2) \log \left[ \frac{\mu_3}{\mu} \right] \right) \end{aligned} \quad (4.50)$$

$$\begin{aligned} m_{2,3d}^2 = & m_2^2 + \frac{1}{24} T^2 (g_2^2 + g_{12}^2) \\ & - \frac{1}{768\pi^2} \left( L_b [24m_1^2 g_{12}^2 + 24m_2^2 g_2^2 + T^2 (-g_2^4 + (g_1^2 + g_2^2) g_{12}^2 - 5g_{12}^4)] \right. \\ & \left. + 4T^2 (g_2^4 + 3g_{12}^4) (\gamma_E - 12 \log A) - 8(3\lambda_{12,3d}^2 + \lambda_{2,3d}^2) \log \left[ \frac{\mu_3}{\mu} \right] \right) \end{aligned} \quad (4.51)$$

$$\phi_{3d} = \phi_1 / \sqrt{T}, \quad (4.52)$$

respectively. Again,  $\mu_3$  is the renormalization scale in the three dimensional theory and  $A \sim 1.2$  is the Glaisher number. It is straight forward to show that the residual scale dependence of  $(\lambda_{1,3d}, \lambda_{2,3d}, \lambda_{12,3d})$  is of  $O(g_i^6)$ . The masses cancel at the same order with the exceptions

$$\mu_3 \frac{\partial m_{1,3d}^2}{\partial \mu_3} = \frac{(g_1^4 + 3g_{12}^4) T^2}{96\pi^2} \quad (4.53)$$

$$\mu_3 \frac{\partial m_{2,3d}^2}{\partial \mu_3} = \frac{(g_2^4 + 3g_{12}^4) T^2}{96\pi^2}. \quad (4.54)$$

The residual scale dependence then for NLO DR is

$$\mu_3 \frac{\partial V_{\text{DR}}}{\partial \mu_3} = - \frac{(g_1^4 \bar{M}_1 + g_2^4 \bar{M}_2 + 3g_{12}^4 (\bar{M}_1 + \bar{M}_2)) T^3}{768\pi^3} \quad (4.55)$$

where

$$\bar{M}_1^2 = m_1^2 + \frac{g_1^2}{2} \phi^2 + \frac{g_1^2 T^2}{24} + \frac{g_{12}^2 T^2}{24}, \quad \bar{M}_2^2 = m_2^2 + \frac{g_2^2}{2} \phi^2 + \frac{g_2^2 T^2}{24} + \frac{g_{12}^2 T^2}{24} \quad (4.56)$$

This again looks to be of similar order as in the single-field case, fourth order in the couplings as opposed to second order for Parwani resummation.

### 4.2.3 Gap resummation

In this model we have to consider two coupled gap equations, one for each scalar field

$$M_1^2 = m_1^2 + \frac{1}{2}g_1^2\phi_1^2 + \frac{g_1^2T^2}{24} + \frac{g_{12}^2T^2}{24} - \frac{g_1^2M_1T}{8\pi} - \frac{g_{12}^2M_2T}{8\pi} - \frac{g_1^2M_1^2L_b}{32\pi^2} - \frac{g_{12}^2M_2^2L_b}{32\pi^2} - \frac{g_1^4L_b\phi_1^2}{32\pi^2} - \frac{g_{12}^4L_b\phi_1^2}{32\pi^2} - \frac{g_1^4T\phi_1^2}{16\pi M_1} - \frac{g_{12}^4T\phi_1^2}{16\pi M_2} \quad (4.57)$$

$$M_2^2 = m_2^2 + \frac{1}{2}g_{12}^2\phi^2 + \frac{g_{12}^2T^2}{24} + \frac{g_2^2T^2}{24} - \frac{g_{12}^2M_1T}{8\pi} - \frac{g_2^2M_2T}{8\pi} - \frac{g_{12}^2L_bM_1^2}{32\pi^2} - \frac{g_2^2L_bM_2^2}{32\pi^2} . \quad (4.58)$$

Excluding the sunset, the one loop tadpole has the form

$$V_1' = \frac{1}{24}g_1^2T^2\phi_1 + \frac{1}{24}g_{12}^2T^2\phi_1 - \frac{g_1^2M_1T\phi_1}{8\pi} - \frac{g_{12}^2M_2\phi_1}{8\pi} - \frac{g_1^2M_1^2\phi_1L_b}{32\pi^2} - \frac{g_{12}^2M_2^2\phi_1L_b}{32\pi^2} . \quad (4.59)$$

Let us first consider the scale dependence of the gap equations up to  $O(g^4)$

$$\mu \frac{dM_1^2}{d\mu} = \frac{g_1^4T^2 + 3g_{12}^4T^2}{192\pi^2} - \frac{3(g_1^4 + g_{12}^4)M_1T + 6g_{12}^4M_2T + 12g_1^4\phi_1^2}{192\pi^3} \quad (4.60)$$

$$\mu \frac{dM_2^2}{d\mu} = \frac{3g_{12}^4T^2 + g_2^4T^2}{192\pi^2} - \frac{3(g_2^4 + g_{12}^4)M_2T + 6g_{12}^4M_1T + 24\pi\phi_1^2}{192\pi^3} . \quad (4.61)$$

The leading terms in the tadpole are

$$\mu \frac{dV_1'}{d\mu} = \frac{(g_1^4 + 3g_{12}^4)T^2\phi_1}{192\pi^2} - \frac{(3g_1^4M_1 + 3g_{12}^4(M_1 + 2M_2))T\phi_1}{192\pi^3} + \mu \frac{dV_{\text{sun}}'}{d\mu} \quad (4.62)$$

It is straight forward to see that the sunset terms cancels the above exactly. The remaining  $O(g_{12}^6)$  term is a little cumbersome, so we omit the explicit expression. However, after integrating, the residual piece is  $O(g_{12}^4/\pi^3)$ , which is the same order the uncanceled piece in dimensional reduction, Eqn. (4.55).

Note again how DR and OPD perform similarly, and both much better than Parwani resummation, with the size of scale dependence parametrically reduced by two powers of the coupling. Our derivation also makes apparent the usability advantage of OPD. Even for this simple toy theory, the OPD calculation is much more tractable than dimensional reduction, and one does not need to take care about whether to use the soft or ultrasoft potential.

## 5 Numerical Implementation of Gap Resummation and Results

We now review how to set up the numerical OPD calculation and how to solve the gap equation away from the origin. In particular, we specify that an iterative approach should be used without any mass derivatives in the gap equation, clarifying some ambiguities from the original numerical treatment [75]. We then present numerical results for the thermal potential and its gravitational wave observables for a representative benchmark point in the two-field  $\phi^4$  theory, comparing OPD and Parwani resummation to demonstrate the improved accuracy and precision of the OPD calculation.

### 5.1 Construction and solution of gap equation away from origin

It is instructive to compare and contrast the numerical implementation of OPD used in this work to that of [75]. Note we restrict ourselves here to the scenario where only one scalar acquires a vev during the phase transition. The general procedure for OPD resummation is as follows:

- We use  $\delta m_i^2$  instead of  $\Pi_i$  to denote corrections to each scalar field's mass beyond the tree level  $m_i^2$ , since it in general includes both zero- and finite-temperature corrections. For a given temperature, the mass corrections  $\delta m_i^2$  are obtained by numerically solving a set of coupled algebraic gap equations on a grid of field values along the excursion of the symmetry breaking field, in this case  $\phi_1$ :

$$\delta m_j^2(\phi_1, T) = \sum_i \left[ \frac{\partial^2 V_{\text{CW}}^i}{\partial \phi_j^2} (m_i^2(\phi_1) + \delta m_i^2(\phi_1, T)) + \frac{\partial^2 V_{\text{th}}^i}{\partial \phi_j^2} (m_i^2(\phi_1) + \delta m_i^2(\phi_1, T)) \right] \quad (5.1)$$

- The continuous functions  $\delta m_j^2(\phi_1, T)$  are obtained from the interpolation of the solutions to the gap equation which are then substituted in the first derivative of the zero + finite temperature 1-loop potential, plus the finite temperature 2-loop sunset term.

$$V_{\text{OPD}} = V_0 + \sum_i \int d\phi_1 \left[ \frac{\partial V_{\text{CW}}^i}{\partial \phi_1} (m_i^2(\phi_1) + \delta m_i^2(\phi_1, T)) + \frac{\partial V_{\text{th}}^i}{\partial \phi_1} (m_i^2(\phi_1) + \delta m_i^2(\phi_1, T)) + \frac{\partial V_{\text{sun}}^i}{\partial \phi_1} (m_i^2(\phi_1) + \delta m_i^2(\phi_1, T)) \right] \quad (5.2)$$

One of the crucial aspects of OPD is its numerical efficiency while going beyond the high-temperature approximation, achieved by using full thermal integrals in the potential but high-temperature approximations in the gap equation.<sup>5</sup> This was justified in [75] by arguing that the gap equation only matters for phase transitions in regions of field- and parameter-space where components of the plasma become light and hence the high-temperature expansion is valid, while further out in field space where the high-temperature expansion fails the thermal mass is accurately treated as small in the full potential, meaning the gap equation has a much smaller effect and its error is parametrically suppressed. As we outline in the next subsection, we have systematically verified that this assumption is in fact correct, justifying the use of the high-temperature expansion in the gap equation and the enormous simplification it brings.

---

<sup>5</sup>Note that the full thermal integrals can be efficiently approximated to high precision by a piecewise defined function joining the high- and low-T approximations, which for the bosonic case is given by  $J_B^{\text{piecewise}}(y^2) = J_B^{\text{high-T}}(y^2) \left[ - \sum_{n=1}^3 \frac{y^2}{n^2} K_2(y n) \right]$  for  $y^2$  less [more] than 0.22, where  $K_2$  is the modified Bessel function of the second kind. We limit  $n \leq 3$  but more precision is easily obtained by including more terms.

$\langle\phi_1\rangle$	400 GeV
$M_{1,\text{pole}}$	125 GeV
$M_{2,\text{pole}}$	600 GeV
$g_{12,\text{phys}}^2$	4.4
$g_{2,\text{phys}}^2$	0.6
$\mu$	600 GeV

**Table 1.** Physical parameters of the two-field model for our benchmark numerical calculation. The fixed value of the renormalization scale  $\mu$  is only used to plot Figs. 1 and 2.

The algebraic equation (5.1) can be solved iteratively:

$$\delta m_j^2(\phi_1, T)_{n+1} = \sum_i \left[ \frac{\partial^2 V_{\text{CW}}^i}{\partial \phi_j^2} (m_i^2(\phi_1) + \delta m_i^2(\phi_1, T)_n) + \frac{\partial^2 V_{\text{th}}^i}{\partial \phi_j^2} (m_i^2(\phi_1) + \delta m_i^2(\phi_1, T)_n) \right] \quad (5.3)$$

for a fixed  $\phi_1$  and  $T$  where the solution starts at  $\delta m_j^2(\phi_1, T)_{n=1} = 0$  and converges to a fixed value after a handful of iterations. However, the authors in [75] found this method of solution to be problematic since it yielded multiple oscillating solutions to the gap equations away from the origin in field space when applied to the SM with simple scalar extensions. This was solved by using an alternative formulation of gap equations which involved keeping mass derivatives in the gap equation and using them to constrain  $\delta m_j(\phi_1 + \Delta\phi_1, T)$  based on the previous solution  $\delta m_j(\phi_1, T)$  on the  $\phi_1$ -grid, turning the algebraic gap equations into a set of differential equations. While this yielded unique and apparently reasonable solutions most of the time, the procedure was very vulnerable to numerical errors due to the singular nature of the resulting gap equation near field values where  $\partial^2 V / \partial \phi_1^2$  flips sign, i.e. when passing through the potential barrier at the critical temperature.

In our careful analysis of OPD as applied to the much simpler two-field  $\phi^4$  theory, we found that the differential version of the gap equation yielded numerical solutions of the effective potential that contained unacceptable artifacts for the sizeable couplings that yield a first order phase transition. On the other hand, the simpler iterative approach always yielded unique and reasonable solutions to the system of gap equations. We therefore use the solution method of Eqn. (5.3) in our analysis.

This is a fortunate development for the application of OPD, since solving the gap equation iteratively is very simple and fast. We hypothesize that the non-convergence of the gap equation solution in [75] was caused by applying OPD to the full SM with extra scalars, without consistently including gauge bosons in the system of gap equations (rather just including their  $\mathcal{O}(T^2)$  contributions in the scalar gap equations). In an upcoming publication we will present an analysis of OPD with the gauge bosons consistently included.

## 5.2 Numerical results for benchmark two-field $\phi^4$ theory

We will now consider the two-field  $\phi^4$  theory with benchmark parameters shown in Table 1, numerically computing the effective potential and gravitational wave signal in Parwani and OPD resummation to compare the two schemes. We find similar behaviour for other

parameter points with strong phase transitions, so these results are representative. As mentioned in the beginning of Sec. 4, this numerical study is done by choosing the  $\overline{\text{MS}}$  parameters at zero temperature for an arbitrary renormalization scale  $\mu$  (chosen to lie near the  $\phi_2$  mass) which reproduces experimental observables at one loop and using these parameters to compute the thermal potential and gravitational signal. This procedure is then repeated for different choices of  $\mu$ . The experimental observables for our model are the vev  $\langle\phi_1\rangle$ , pole mass  $M_1, M_2$  of the scalar fields at the symmetry broken vacuum and the quartic couplings  $g_{12}^2$  and  $g_2^2$ . The details of the one loop matching of the parameters to the experimental observables are given in Appendix A.

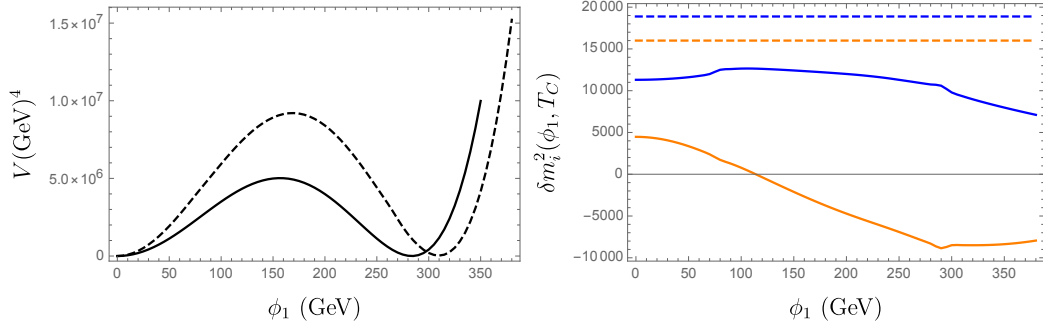


**Figure 1.** Left panel: the effective potential with one loop matching for the benchmark in Table 1 and  $\mu = 600$  GeV with the solid line denoting OPD and the dashed line referring to Parwani resummation. Right panel: numerical solution of the gap equation for the mass correction  $\delta m_i^2(\phi_1, T_c)$  at the critical temperature for the same benchmark. The orange and blue curves are for  $\phi_1$  and  $\phi_2$  respectively.

Fig. 1 shows the thermal potential for our benchmark point at  $T = T_c$  when the true and false minima are degenerate, as well as the corresponding solutions to the gap equation. As one can see the iterative method does give a smooth, unique solution exhibiting correct physical behavior, whereby the mass corrections are maximum at the origin and decreases with  $\langle\phi_1\rangle$  since the fields acquire more mass reducing their participation in the thermal plasma. This is markedly different from the constant thermal masses assumed in Parwani resummation, which makes use of the lowest-order high-temperature expansion far away from the origin where it is no longer justified.

On the other hand, we also verified, for this and other choices of parameters, that the use of the high-T expansion in the gap equation for OPD was valid. Compared to solving the gap equations with full thermal functions, we only found meaningful differences in the region of field space where  $M^2/T^2$  is large,  $M^2$  being the resummed mass. For example, for this particular benchmark this difference shows up when  $M_2^2/T^2 \gtrsim 3$ , significantly larger than the still sizeable but more moderate values relevant for our phase transition. Even then, the difference in  $\delta m_i^2$  (full thermal potential) obtained with the high-temperature approximation in the gap equation vs full thermal functions in the gap equations are at most  $\sim 10\%$  (1%). This confirms the original argument for the high-temperature approximation in the gap equation made in [75].

OPD by construction is more accurate as it takes into account both proper counting of

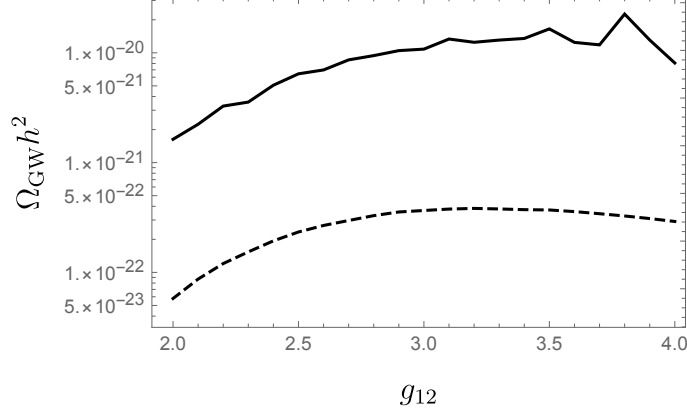


**Figure 2.** The maximal gravitational wave amplitude for all parameters fixed except  $g_{12}$ . Solid line denotes the prediction of OPD and dashed line the predictions of Parwani.

diagrams and higher order corrections. These higher order corrections do make a significant change in the profile of the thermal potential. OPD seems to predict a larger barrier for the thermal potential when compared to TFD as seen in fig. 1. This tends to be a general feature of OPD throughout the parameter space and results in the maximal gravitational wave amplitude being orders of magnitude larger than what is predicted by TFD as can be seen in fig. 2.

In addition to better accuracy, the numerical results also demonstrates significantly improved precision, as signaled by the reduction of scale dependence when using OPD. Figs. 3 and 4 show the variation of the thermal parameters and peak gravitational wave amplitude as a function of the renormalization scale. An estimate of the variation of the critical and percolation temperature,  $\Delta T = \frac{T_{\text{max}} - T_{\text{min}}}{T_{\text{max}}}$  on varying the renormalization scale gives  $\Delta T_{\text{OPD}} \sim 2\%$  compared to  $\Delta T_{\text{TFD}} \sim 15\%$ . Similarly, almost a factor of 1.7 reduction is observed in the variation of the strength of the phase transition,  $\Delta\alpha$  with  $\Delta\alpha_{\text{TFD}} \sim 49\%$  and  $\Delta\alpha_{\text{OPD}} \sim 29\%$ . Of course, it is to be noted that not all the thermal observables show such an improvement. In particular it can be seen in fig. 3 that  $\phi_c$  has a larger variation in OPD ( $\Delta\phi_{c,\text{OPD}} \sim 12.6\%$ ) compared to TFD ( $\Delta\phi_{c,\text{TFD}} \sim 3.4\%$ ). This on the other hand has minimal effect on variation of the gravitational wave observables since both  $\alpha$  and  $\beta/H_*$  have stronger dependence on  $T_p$  rather than  $\phi_c$ . In particular, this also means that OPD's prediction of the gravitational wave peak frequency has much better precision. While the results here show the superiority of OPD compared to TFD, one should note that in a realistic model one would expect even better scale dependence. This is due to the fact that to achieve a first order phase transition in this model, a very large  $g_{12}$  coupling is required to compensate for the small number of degrees of freedom that become massive during the transition. The portal coupling is so large that the uncertainty from matching is significant, despite this being a zero temperature uncertainty. This is an unfortunate artifact of the toy model we used to develop this analysis. The  $\mu$  dependent lines for the thermal parameters are almost in parallel, demonstrating that as we are near the non-perturbative regime where zero temperature uncertainties are nearly out of control,

even if the finite temperature uncertainties are greatly improved by the OPD resummation scheme.

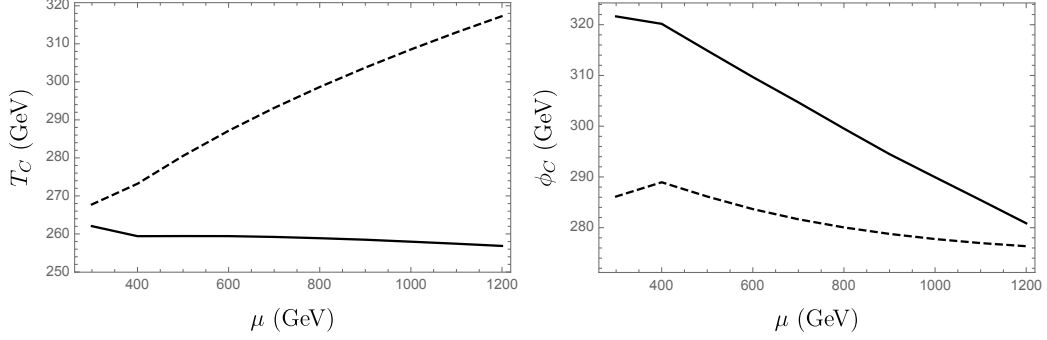


**Figure 3.** The scale dependence ( $\mu$ ) of the critical temperature and vev for the benchmark in Table 1 with solid line corresponding to Parwani and dashed line corresponding to OPD with both augmented by 2 loop sunsets.

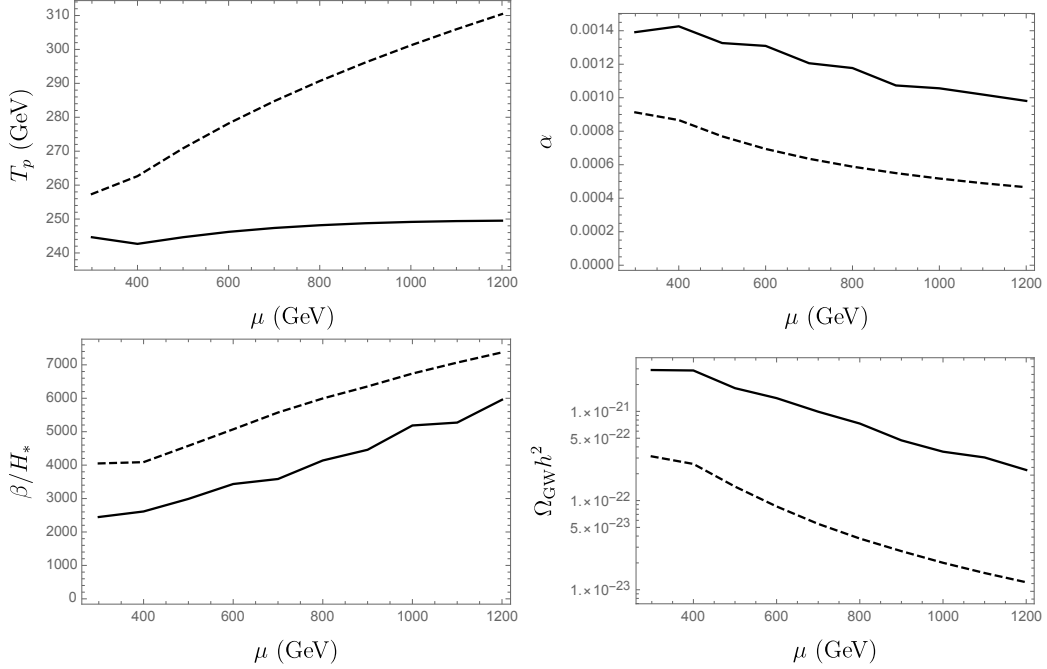


**Figure 4.** The scale dependence ( $\mu$ ) of the thermal parameters and the peak gravitational wave amplitude as predicted by the sound shell model. Solid and dashed line correspond to Parwani and OPD respectively.

Finally, as a last check we should also compare the results to that of dimensional reduction. Unfortunately due to the large couplings involved the high temperature expansion for  $M_2$  badly breaks down near the critical temperature. This makes the use of standard forms of dimensional reduction inappropriate. Particularly problematic is the two loop sunset diagram that scales as  $\phi^2 T^2$  times a large logarithm in the high temperature expan-

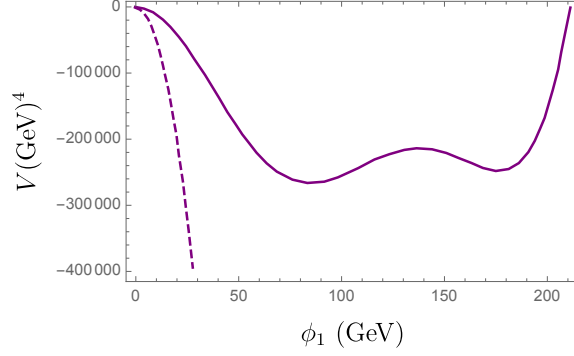


**Figure 5.** Soft potential in NLO dimensional reduction using the benchmark in table 1 (solid purple) at  $T = 191.7$  GeV as well as the problematic HT calculation of the 2 loop sunset which dominates (dashed purple).

sion (see the last line of equation 4.46). This term actually dominates when not Boltzmann suppressed and is responsible for the double barrier behaviour we see in fig. 5. Note the ultrasoft potential does not do better as it is actually unbounded (and contains strange kinks).

## 6 Discussion and conclusion

Understanding the era of cosmological electroweak symmetry is a central question of the next generation of theoretical and experimental efforts. Conventional methods of modelling cosmological electroweak symmetry breaking suffer very difficult theoretical uncertainties. Accurate calculations involving next to leading order dimensional reduction are very difficult and, to this day, there exists no global treatment of a BSM scenario involving extra dynamical scalar fields. Further, off the shelf dimensional reduction is in the high temperature regime, whereas strong phase transitions catalyzed by thermally induced barriers necessitates large couplings where the high temperature regime is expected to be invalid.

In the context of all of these issues, we are motivated to investigate and further develop the OPD scheme utilizing a recursive solution to the gap equation for scalar masses (though it is worth keeping in mind that the solution of the gap equation can also be used as a replacement for calculating the self energy used in matching relations in the dimensional reduction paradigm as well). OPD includes sizeable contributions neglected by the Parwani scheme, and is therefore required for more accurate calculations. In the context of theoretical uncertainties, our results seem to suggest regions for cautious optimism with regard to OPD. The analytic calculation in Sec. 4 indicates a similar precision, i.e. scale dependence at fourth coupling order, to dimensional reduction, improving on the second-order dependence of Parwani resummation, while the ease of going beyond the high-temperature approximation in OPD promises additional advantages for phase transitions with sizeable couplings. Numerical results in Sec. 5 for the thermal parameters show an improvement for OPD compared to TFD, giving further grounds for optimism. All of the thermal parameters except the critical vev display significant reduction in theoretical uncertainty when



using OPD. This anomalous behavior for the critical vev does not significantly influence the final gravitational result due to larger dependence on the other thermal parameters, and at any rate we suspect that this is an artifact of the very large couplings necessary for a strong phase transition in our toy model.

Our study represents a first step in a systematic and rigorous development of the OPD scheme for precision high-temperature calculations, and there is a clear itinerary of future directions that must be pursued to apply OPD to realistic extensions of the SM. The highest priority next steps include understanding the importance of full momentum dependent self-energy in gap equations, consistent inclusion of gauge bosons in the system of gap equations, and addition of sunset equivalent diagrams in the gauge sector; as well as appropriate modification to the gap equation for multiple symmetry broken fields to handle arbitrary field excursions during the phase transition. This will allow a careful examination of how OPD could be combined with renormalization group improvement of the zero-temperature potential to further reduce the theoretical uncertainties. Finally, being able to include non-renormalizable operators would be very useful, given the importance of SMEFT to constrain BSM physics at colliders and elsewhere. We are currently working to address these issues and plan to present them in a future publication.

**Acknowledgements:** We would like to thank Phillipp Schicho for help with DRalgo and Johan Löfgren for useful comment about the zero-momentum approximation of the self energy in the gap equation. The research of DC was supported in part by a Discovery Grant from the Natural Sciences and Engineering Research Council of Canada, the Canada Research Chair program, the Alfred P. Sloan Foundation, the Ontario Early Researcher Award, and the University of Toronto McLean Award. The research of JR was supported in part by the Natural Science and Engineering Research Council of Canada. The work of GW is supported by World Premier International Research Center Initiative (WPI), MEXT, Japan. GW was supported by JSPS KAKENHI Grant Number JP22K14033.

## A Loop level matching

For the matching calculation, we relate the following physical input parameters to the  $\overline{\text{MS}}$  Lagrangian parameters at one loop.

$$(\phi_c, M_{1,\text{pole}}, M_{2,\text{pole}}, g_{12,\text{phys}}, g_{2,\text{phys}}) \longmapsto (\mu_1, m_2, g_1, g_{12}, g_2) \quad (\text{A.1})$$

For loop level matching, the standard one-loop renormalization of the tadpole and the self energy diagrams at zero temperature gives three of the conditions relating the physical input parameters to the Lagrangian parameters

$$V'_1(\phi_c) = 0 \quad (\text{A.2})$$

$$m_1^2(\phi_c) = M_{1,\text{pole}}^2 + \Pi_1(M_{1,\text{pole}}^2) \quad (\text{A.3})$$

$$m_2^2(\phi_c) = M_{2,\text{pole}}^2 + \Pi_2(M_{2,\text{pole}}^2) \quad (\text{A.4})$$

where  $V_1$  is the 1-loop potential,  $m_1^2(\phi_c) = -\mu_1^2 + \frac{1}{2}g_1^2\phi_c^2$ ,  $m_2^2(\phi_c) = m_2^2 + \frac{1}{2}g_{12}^2\phi_c^2$  are the field dependent masses and the functions can be written in terms of the Lagrangian parameters

$$V_1'(\phi_c) = -\mu_1^2 + \frac{1}{6}g_1^2\phi_c^2 - \frac{g_1^2 m_1^2(\phi_c)}{32\pi^2} \left( \log \left[ \frac{\mu^2}{m_1^2(\phi_c)} \right] + 1 \right) - \frac{g_{12}^2 m_2^2(\phi_c)}{32\pi^2} \left( \log \left[ \frac{\mu^2}{m_2^2(\phi_c)} \right] + 1 \right) \quad (\text{A.5})$$

$$\begin{aligned} \Pi_1(p^2) = & \frac{g_1^2 m_1^2(\phi_c)}{32\pi^2} \left( \log \left[ \frac{\mu^2}{m_1^2(\phi_c)} \right] + 1 \right) + \frac{g_{12}^2 m_2^2(\phi_c)}{32\pi^2} \left( \log \left[ \frac{\mu^2}{m_2^2(\phi_c)} \right] + 1 \right) \\ & + \frac{g_1^4 \phi_c^2}{32\pi^2} \left( \frac{\sqrt{p^2(p^2 - 4m_1^2(\phi_c))}}{p^2} \log \left[ \frac{2m_1^2(\phi_c) + \sqrt{p^2(p^2 - 4m_1^2(\phi_c))} - p^2}{2m_1^2(\phi_c)} \right] \right. \\ & + \log \left[ \frac{\mu^2}{m_1^2(\phi_c)} \right] + 2 \Big) + \frac{g_{12}^4 \phi_c^2}{32\pi^2} \left( 2 + \log \left[ \frac{\mu^2}{m_2^2(\phi_c)} \right] \right. \\ & \left. + \frac{\sqrt{p^2(p^2 - 4m_2^2(\phi_c))}}{p^2} \log \left[ \frac{\sqrt{p^2(p^2 - 4m_2^2(\phi_c))} + 2m_2^2(\phi_c) - p^2}{2m_2^2(\phi_c)} \right] \right) \end{aligned} \quad (\text{A.6})$$

$$\begin{aligned} \Pi_2(p^2) = & \frac{g_{12}^2 m_1^2(\phi_c)}{32\pi^2} \left( \log \left[ \frac{\mu^2}{m_1^2(\phi_c)} \right] + 1 \right) + \frac{g_2^2 m_2^2(\phi_c)}{32\pi^2} \left( \log \left[ \frac{\mu^2}{m_2^2(\phi_c)} \right] + 1 \right) \\ & + \frac{g_{12}^4 \phi_c^2}{16\pi^2} \left( -\frac{(m_1^2(\phi_c) - m_2^2(\phi_c) + p^2)}{2p^2} \log \left[ \frac{m_1^2(\phi_c)}{m_2^2(\phi_c)} \right] \right. \\ & + \frac{\sqrt{(m_1^2(\phi_c) - m_2^2(\phi_c))^2 - 2p^2(m_1^2(\phi_c) + m_2^2(\phi_c)) + p^4}}{p^2} \\ & \times \log \left[ \frac{\sqrt{(m_1^2(\phi_c) - m_2^2(\phi_c))^2 - 2p^2(m_1^2(\phi_c) + m_2^2(\phi_c)) + p^4} + m_1^2(\phi_c) + m_2^2(\phi_c) - p^2}{2m_1(\phi_c)m_2(\phi_c)} \right] \\ & \left. + \log \left[ \frac{\mu^2}{m_2^2(\phi_c)} \right] + 2 \right) \end{aligned} \quad (\text{A.7})$$

Note that for loop level matching the masses are not obtained by taking the second of the 1-loop potential since these correspond to zero external momentum while the pole masses lie at nonzero external momentum. Finally the remaining two conditions come from the one-loop renormalization of the four point function at zero external momentum. These can be obtained from the derivatives of the 1-loop potential which is the tree plus Coleman-Weinberg potential.

$$g_{12,\text{phys}}^2 = \left. \frac{\partial^4 V_1}{\partial \phi_1^2 \partial \phi_2^2} \right|_{(\phi_1, \phi_2) = (\phi_c, 0)} \quad (\text{A.8})$$

$$g_{2,\text{phys}}^2 = \left. \frac{\partial^4 V_1}{\partial \phi_2^4} \right|_{(\phi_1, \phi_2) = (\phi_c, 0)} \quad (\text{A.9})$$

## B 2-loop Sunset diagram

The full expression of sunset diagrams used in our results have been calculated in [65, 91]

$$V_{\text{sun}} = -\frac{g^4 \phi^2}{12} (G_0(m^2) + G_1(m^2, T) + G_2(m^2, T)) \quad (\text{B.1})$$

where

$$G_0(m^2) = -\frac{3m^2}{2(4\pi)^4} \left( \log^2 \left[ \frac{\mu^2}{m^2} \right] + 4 \log \left[ \frac{\mu^2}{m^2} \right] + 4 + \frac{\pi^2}{6} - \frac{8.966523919}{3} \right) \quad (\text{B.2})$$

$$G_1(m^2, T) = \frac{3}{(4\pi)^2} \left( \log \left[ \frac{\mu^2}{m^2} \right] + 2 \right) \int \frac{d^3 q}{(2\pi)^3} \frac{n_B(q)}{\omega_q} \\ + \frac{3}{4(2\pi)^4} \int_0^\infty dq_1 \frac{q_1 n_B(q_1)}{\omega_{q_1}} \int_0^\infty \frac{dq_2}{\omega_{q_2}} \left( q_2 \log \left| \frac{X_+}{X_-} \right| - q_1 \right) \quad (\text{B.3})$$

with

$$X_\pm = (\omega_{q_1} + \omega_{q_2} + \omega_{q_1 \pm q_2})^2 \times (-\omega_{q_1} + \omega_{q_2} + \omega_{q_1 \pm q_2})^2 \quad (\text{B.4})$$

$$G_2(m^2, T) = \frac{3}{4(2\pi)^4} \int_0^\infty dq_1 \frac{q_1 n_B(q_1)}{\omega_{q_1}} \int_0^\infty dq_2 \frac{q_2 n_B(q_2)}{\omega_{q_2}} \log \left| \frac{Y_+}{Y_-} \right| \quad (\text{B.5})$$

with

$$Y_\pm = (\omega_{q_1} + \omega_{q_2} + \omega_{q_1 \pm q_2})^2 \times (-\omega_{q_1} + \omega_{q_2} + \omega_{q_1 \pm q_2})^2 \\ \times (\omega_{q_1} - \omega_{q_2} + \omega_{q_1 \pm q_2})^2 \times (\omega_{q_1} + \omega_{q_2} - \omega_{q_1 \pm q_2})^2 \quad (\text{B.6})$$

Here  $G_0$  is the pure zero-temperature piece while  $G_1, G_2$  are the finite temperature pieces. The latter terms are included in the 4D perturbative schemes since at high temperature their contributions are the same as 1-loop contributions.

## References

- [1] D. Curtin, P. Meade and C.-T. Yu, *Testing Electroweak Baryogenesis with Future Colliders*, *JHEP* **11** (2014) 127 [[1409.0005](#)].
- [2] A.V. Kotwal, M.J. Ramsey-Musolf, J.M. No and P. Winslow, *Singlet-catalyzed electroweak phase transitions in the 100 TeV frontier*, *Phys. Rev. D* **94** (2016) 035022 [[1605.06123](#)].
- [3] M.J. Ramsey-Musolf, *The electroweak phase transition: a collider target*, *JHEP* **09** (2020) 179 [[1912.07189](#)].
- [4] A. Papaefstathiou and G. White, *The electro-weak phase transition at colliders: confronting theoretical uncertainties and complementary channels*, *JHEP* **05** (2021) 099 [[2010.00597](#)].
- [5] M. Trodden, *Electroweak baryogenesis: A Brief review*, in *33rd Rencontres de Moriond: Electroweak Interactions and Unified Theories*, pp. 471–480, 1998 [[hep-ph/9805252](#)].
- [6] J.M. Cline, *Baryogenesis*, in *Les Houches Summer School - Session 86: Particle Physics and Cosmology: The Fabric of Spacetime*, 9, 2006 [[hep-ph/0609145](#)].
- [7] D.E. Morrissey and M.J. Ramsey-Musolf, *Electroweak baryogenesis*, *New J. Phys.* **14** (2012) 125003 [[1206.2942](#)].

- [8] G.A. White, *A Pedagogical Introduction to Electroweak Baryogenesis*, .
- [9] B. Garbrecht, *Why is there more matter than antimatter? Computational methods for leptogenesis and electroweak baryogenesis*, *Prog. Part. Nucl. Phys.* **110** (2020) 103727 [[1812.02651](#)].
- [10] S. Profumo, M.J. Ramsey-Musolf and G. Shaughnessy, *Singlet Higgs phenomenology and the electroweak phase transition*, *JHEP* **08** (2007) 010 [[0705.2425](#)].
- [11] C. Delaunay, C. Grojean and J.D. Wells, *Dynamics of Non-renormalizable Electroweak Symmetry Breaking*, *JHEP* **04** (2008) 029 [[0711.2511](#)].
- [12] P. Huang, A.J. Long and L.-T. Wang, *Probing the Electroweak Phase Transition with Higgs Factories and Gravitational Waves*, *Phys. Rev. D* **94** (2016) 075008 [[1608.06619](#)].
- [13] M. Chala, C. Krause and G. Nardini, *Signals of the electroweak phase transition at colliders and gravitational wave observatories*, *JHEP* **07** (2018) 062 [[1802.02168](#)].
- [14] D. Croon, O. Gould, P. Schicho, T.V.I. Tenkanen and G. White, *Theoretical uncertainties for cosmological first-order phase transitions*, *JHEP* **04** (2021) 055 [[2009.10080](#)].
- [15] C. Grojean and G. Servant, *Gravitational Waves from Phase Transitions at the Electroweak Scale and Beyond*, *Phys. Rev. D* **75** (2007) 043507 [[hep-ph/0607107](#)].
- [16] A. Alves, T. Ghosh, H.-K. Guo, K. Sinha and D. Vagie, *Collider and Gravitational Wave Complementarity in Exploring the Singlet Extension of the Standard Model*, *JHEP* **04** (2019) 052 [[1812.09333](#)].
- [17] A. Alves, D. Gonçalves, T. Ghosh, H.-K. Guo and K. Sinha, *Di-Higgs Blind Spots in Gravitational Wave Signals*, *Phys. Lett. B* **818** (2021) 136377 [[2007.15654](#)].
- [18] V. Vaskonen, *Electroweak baryogenesis and gravitational waves from a real scalar singlet*, *Phys. Rev. D* **95** (2017) 123515 [[1611.02073](#)].
- [19] G.C. Dorsch, S.J. Huber, T. Konstandin and J.M. No, *A Second Higgs Doublet in the Early Universe: Baryogenesis and Gravitational Waves*, *JCAP* **05** (2017) 052 [[1611.05874](#)].
- [20] W. Chao, H.-K. Guo and J. Shu, *Gravitational Wave Signals of Electroweak Phase Transition Triggered by Dark Matter*, *JCAP* **09** (2017) 009 [[1702.02698](#)].
- [21] X. Wang, F.P. Huang and X. Zhang, *Gravitational wave and collider signals in complex two-Higgs doublet model with dynamical CP-violation at finite temperature*, *Phys. Rev. D* **101** (2020) 015015 [[1909.02978](#)].
- [22] S.V. Demidov, D.S. Gorbunov and D.V. Kirpichnikov, *Gravitational waves from phase transition in split NMSSM*, *Phys. Lett. B* **779** (2018) 191 [[1712.00087](#)].
- [23] A. Ahriche, K. Hashino, S. Kanemura and S. Nasri, *Gravitational Waves from Phase Transitions in Models with Charged Singlets*, *Phys. Lett. B* **789** (2019) 119 [[1809.09883](#)].
- [24] F.P. Huang and J.-H. Yu, *Exploring inert dark matter blind spots with gravitational wave signatures*, *Phys. Rev. D* **98** (2018) 095022 [[1704.04201](#)].
- [25] A. Mohamadnejad, *Gravitational waves from scale-invariant vector dark matter model: Probing below the neutrino-floor*, *Eur. Phys. J. C* **80** (2020) 197 [[1907.08899](#)].
- [26] I. Baldes and G. Servant, *High scale electroweak phase transition: baryogenesis \& symmetry non-restoration*, *JHEP* **10** (2018) 053 [[1807.08770](#)].

- [27] F.P. Huang, Z. Qian and M. Zhang, *Exploring dynamical CP violation induced baryogenesis by gravitational waves and colliders*, *Phys. Rev. D* **98** (2018) 015014 [[1804.06813](#)].
- [28] S.A.R. Ellis, S. Ipek and G. White, *Electroweak Baryogenesis from Temperature-Varying Couplings*, *JHEP* **08** (2019) 002 [[1905.11994](#)].
- [29] A. Alves, T. Ghosh, H.-K. Guo and K. Sinha, *Resonant Di-Higgs Production at Gravitational Wave Benchmarks: A Collider Study using Machine Learning*, *JHEP* **12** (2018) 070 [[1808.08974](#)].
- [30] A. Alves, D. Gonçalves, T. Ghosh, H.-K. Guo and K. Sinha, *Di-Higgs Production in the 4b Channel and Gravitational Wave Complementarity*, *JHEP* **03** (2020) 053 [[1909.05268](#)].
- [31] J.M. Cline, A. Friedlander, D.-M. He, K. Kainulainen, B. Laurent and D. Tucker-Smith, *Baryogenesis and gravity waves from a UV-completed electroweak phase transition*, *Phys. Rev. D* **103** (2021) 123529 [[2102.12490](#)].
- [32] W. Chao, H.-K. Guo and X.-F. Li, *First Order Color Symmetry Breaking and Restoration Triggered by Electroweak Symmetry Non-restoration*, [2112.13580](#).
- [33] J. Liu, X.-P. Wang and K.-P. Xie, *Searching for lepton portal dark matter with colliders and gravitational waves*, *JHEP* **06** (2021) 149 [[2104.06421](#)].
- [34] Z. Zhang, C. Cai, X.-M. Jiang, Y.-L. Tang, Z.-H. Yu and H.-H. Zhang, *Phase transition gravitational waves from pseudo-Nambu-Goldstone dark matter and two Higgs doublets*, *JHEP* **05** (2021) 160 [[2102.01588](#)].
- [35] R.-G. Cai, K. Hashino, S.-J. Wang and J.-H. Yu, *Gravitational waves from patterns of electroweak symmetry breaking: an effective perspective*, [2202.08295](#).
- [36] C. Caprini et al., *Detecting gravitational waves from cosmological phase transitions with LISA: an update*, *JCAP* **03** (2020) 024 [[1910.13125](#)].
- [37] M. Punturo et al., *The Einstein Telescope: A third-generation gravitational wave observatory*, *Class. Quant. Grav.* **27** (2010) 194002.
- [38] K. Yagi and N. Seto, *Detector configuration of DECIGO/BBO and identification of cosmological neutron-star binaries*, *Phys. Rev. D* **83** (2011) 044011 [[1101.3940](#)].
- [39] AEDGE collaboration, *AEDGE: Atomic Experiment for Dark Matter and Gravity Exploration in Space*, *EPJ Quant. Technol.* **7** (2020) 6 [[1908.00802](#)].
- [40] S. Hild et al., *Sensitivity Studies for Third-Generation Gravitational Wave Observatories*, *Class. Quant. Grav.* **28** (2011) 094013 [[1012.0908](#)].
- [41] A. Sesana et al., *Unveiling the gravitational universe at  $\mu$ -Hz frequencies*, *Exper. Astron.* **51** (2021) 1333 [[1908.11391](#)].
- [42] THEIA collaboration, *Theia: Faint objects in motion or the new astrometry frontier*, [1707.01348](#).
- [43] P. Schwaller, *Gravitational Waves from a Dark Phase Transition*, *Phys. Rev. Lett.* **115** (2015) 181101 [[1504.07263](#)].
- [44] I. Baldes and C. Garcia-Cely, *Strong gravitational radiation from a simple dark matter model*, *JHEP* **05** (2019) 190 [[1809.01198](#)].
- [45] M. Breitbach, J. Kopp, E. Madge, T. Opferkuch and P. Schwaller, *Dark, Cold, and Noisy: Constraining Secluded Hidden Sectors with Gravitational Waves*, *JCAP* **07** (2019) 007 [[1811.11175](#)].

- [46] D. Croon, V. Sanz and G. White, *Model Discrimination in Gravitational Wave spectra from Dark Phase Transitions*, *JHEP* **08** (2018) 203 [[1806.02332](#)].
- [47] E. Hall, T. Konstandin, R. McGehee, H. Murayama and G. Servant, *Baryogenesis From a Dark First-Order Phase Transition*, *JHEP* **04** (2020) 042 [[1910.08068](#)].
- [48] I. Baldes, *Gravitational waves from the asymmetric-dark-matter generating phase transition*, *JCAP* **05** (2017) 028 [[1702.02117](#)].
- [49] M. Geller, A. Hook, R. Sundrum and Y. Tsai, *Primordial Anisotropies in the Gravitational Wave Background from Cosmological Phase Transitions*, *Phys. Rev. Lett.* **121** (2018) 201303 [[1803.10780](#)].
- [50] D. Croon, A. Kusenko, A. Mazumdar and G. White, *Solitonsynthesis and Gravitational Waves*, *Phys. Rev. D* **101** (2020) 085010 [[1910.09562](#)].
- [51] E. Hall, T. Konstandin, R. McGehee and H. Murayama, *Asymmetric Matters from a Dark First-Order Phase Transition*, [1911.12342](#).
- [52] W. Chao, X.-F. Li and L. Wang, *Filtered pseudo-scalar dark matter and gravitational waves from first order phase transition*, *JCAP* **06** (2021) 038 [[2012.15113](#)].
- [53] J.B. Dent, B. Dutta, S. Ghosh, J. Kumar and J. Runburg, *Sensitivity to dark sector scales from gravitational wave signatures*, *JHEP* **08** (2022) 300 [[2203.11736](#)].
- [54] K. Hashino, M. Kakizaki, S. Kanemura, P. Ko and T. Matsui, *Gravitational waves from first order electroweak phase transition in models with the  $U(1)_X$  gauge symmetry*, *JHEP* **06** (2018) 088 [[1802.02947](#)].
- [55] F.P. Huang and X. Zhang, *Probing the gauge symmetry breaking of the early universe in 3-3-1 models and beyond by gravitational waves*, *Phys. Lett. B* **788** (2019) 288 [[1701.04338](#)].
- [56] D. Croon, T.E. Gonzalo and G. White, *Gravitational Waves from a Pati-Salam Phase Transition*, *JHEP* **02** (2019) 083 [[1812.02747](#)].
- [57] V. Brdar, L. Graf, A.J. Helmboldt and X.-J. Xu, *Gravitational Waves as a Probe of Left-Right Symmetry Breaking*, *JCAP* **12** (2019) 027 [[1909.02018](#)].
- [58] W.-C. Huang, F. Sannino and Z.-W. Wang, *Gravitational Waves from Pati-Salam Dynamics*, *Phys. Rev. D* **102** (2020) 095025 [[2004.02332](#)].
- [59] T. Prokopec, J. Rezacek and B. Świeżewska, *Gravitational waves from conformal symmetry breaking*, *JCAP* **02** (2019) 009 [[1809.11129](#)].
- [60] M. Kierkla, A. Karam and B. Swieżewska, *Conformal model for gravitational waves and dark matter: A status update*, [2210.07075](#).
- [61] R. Caldwell et al., *Detection of Early-Universe Gravitational Wave Signatures and Fundamental Physics*, [2203.07972](#).
- [62] P. Schicho, T.V.I. Tenkanen and G. White, *Combining thermal resummation and gauge invariance for electroweak phase transition*, [2203.04284](#).
- [63] A.D. Linde, *Infrared Problem in Thermodynamics of the Yang-Mills Gas*, *Phys. Lett. B* **96** (1980) 289.
- [64] P.B. Arnold, *Phase transition temperatures at next-to-leading order*, *Phys. Rev. D* **46** (1992) 2628 [[hep-ph/9204228](#)].

- [65] R.R. Parwani, *Resummation in a hot scalar field theory*, *Phys. Rev. D* **45** (1992) 4695 [[hep-ph/9204216](#)].
- [66] O. Gould and T.V.I. Tenkanen, *On the perturbative expansion at high temperature and implications for cosmological phase transitions*, *JHEP* **06** (2021) 069 [[2104.04399](#)].
- [67] A. Ekstedt, O. Gould and J. Löfgren, *Radiative first-order phase transitions to next-to-next-to-leading order*, *Phys. Rev. D* **106** (2022) 036012 [[2205.07241](#)].
- [68] O. Gould, S. Güyer and K. Rummukainen, *First-order electroweak phase transitions: a nonperturbative update*, [2205.07238](#).
- [69] A. Ekstedt, P. Schicho and T.V.I. Tenkanen, *DRalgo: a package for effective field theory approach for thermal phase transitions*, [2205.08815](#).
- [70] C.G. Boyd, D.E. Brahm and S.D.H. Hsu, *Resummation methods at finite temperature: The Tadpole way*, *Phys. Rev. D* **48** (1993) 4963 [[hep-ph/9304254](#)].
- [71] J.R. Espinosa, M. Quiros and F. Zwirner, *On the phase transition in the scalar theory*, *Phys. Lett. B* **291** (1992) 115 [[hep-ph/9206227](#)].
- [72] J.R. Espinosa, M. Quiros and F. Zwirner, *On the nature of the electroweak phase transition*, *Phys. Lett. B* **314** (1993) 206 [[hep-ph/9212248](#)].
- [73] M. Dine, R.G. Leigh, P.Y. Huet, A.D. Linde and D.A. Linde, *Towards the theory of the electroweak phase transition*, *Phys. Rev. D* **46** (1992) 550 [[hep-ph/9203203](#)].
- [74] C.G. Boyd, D.E. Brahm and S.D.H. Hsu, *Corrections to the electroweak effective action at finite temperature*, *Phys. Rev. D* **48** (1993) 4952 [[hep-ph/9206235](#)].
- [75] D. Curtin, P. Meade and H. Ramani, *Thermal Resummation and Phase Transitions*, *Eur. Phys. J. C* **78** (2018) 787 [[1612.00466](#)].
- [76] W. Buchmüller and O. Philipsen, *Phase structure and phase transition of the  $SU(2)$  Higgs model in three-dimensions*, *Nucl. Phys. B* **443** (1995) 47 [[hep-ph/9411334](#)].
- [77] F. Gao and I.M. Oldengott, *Cosmology meets functional QCD: First-order cosmic QCD transition induced by large lepton asymmetries*, [2106.11991](#).
- [78] J. Ellis, M. Lewicki and J.M. No, *On the Maximal Strength of a First-Order Electroweak Phase Transition and its Gravitational Wave Signal*, *JCAP* **04** (2019) 003 [[1809.08242](#)].
- [79] J. Ellis, M. Lewicki, J.M. No and V. Vaskonen, *Gravitational wave energy budget in strongly supercooled phase transitions*, *JCAP* **06** (2019) 024 [[1903.09642](#)].
- [80] H.-K. Guo, K. Sinha, D. Vagie and G. White, *Phase Transitions in an Expanding Universe: Stochastic Gravitational Waves in Standard and Non-Standard Histories*, *JCAP* **01** (2021) 001 [[2007.08537](#)].
- [81] C. Gowling, M. Hindmarsh, D.C. Hooper and J. Torrado, *Reconstructing physical parameters from template gravitational wave spectra at LISA: first order phase transitions*, [2209.13551](#).
- [82] M. Quiros, *Field theory at finite temperature and phase transitions*, *Helv. Phys. Acta* **67** (1994) 451.
- [83] K. Kajantie, M. Laine, K. Rummukainen and M.E. Shaposhnikov, *Generic rules for high temperature dimensional reduction and their application to the standard model*, *Nucl. Phys. B* **458** (1996) 90 [[hep-ph/9508379](#)].

- [84] M. Hindmarsh, S.J. Huber, K. Rummukainen and D.J. Weir, *Gravitational waves from the sound of a first order phase transition*, *Phys. Rev. Lett.* **112** (2014) 041301 [[1304.2433](#)].
- [85] M. Hindmarsh, S.J. Huber, K. Rummukainen and D.J. Weir, *Numerical simulations of acoustically generated gravitational waves at a first order phase transition*, *Phys. Rev. D* **92** (2015) 123009 [[1504.03291](#)].
- [86] M. Hindmarsh, S.J. Huber, K. Rummukainen and D.J. Weir, *Shape of the acoustic gravitational wave power spectrum from a first order phase transition*, *Phys. Rev. D* **96** (2017) 103520 [[1704.05871](#)].
- [87] M. Hindmarsh and M. Hijazi, *Gravitational waves from first order cosmological phase transitions in the Sound Shell Model*, *JCAP* **12** (2019) 062 [[1909.10040](#)].
- [88] H.-K. Guo, K. Sinha, D. Vagie and G. White, *The benefits of diligence: how precise are predicted gravitational wave spectra in models with phase transitions?*, *JHEP* **06** (2021) 164 [[2103.06933](#)].
- [89] C. Gowling and M. Hindmarsh, *Observational prospects for phase transitions at LISA: Fisher matrix analysis*, *JCAP* **10** (2021) 039 [[2106.05984](#)].
- [90] F. Giese, T. Konstandin and J. van de Vis, *Finding sound shells in LISA mock data using likelihood sampling*, *JCAP* **11** (2021) 002 [[2107.06275](#)].
- [91] G. Smet, T. Vanzieleghem, K. Van Acoleyen and H. Verschelde, *Two-loop two-particle point irreducible analysis of  $\lambda\varphi^4$  theory at finite temperature*, *Phys. Rev. D* **65** (2002) 045015.